Landscape Ecol (2016) 31:2045–2062
DOI 10.1007/s10980-016-0381-y

RESEARCH ARTICLE

Effect of spatial image support in detecting long-term vegetation change from satellite time-series

Jonathan J. Maynard · Jason W. Karl · Dawn M. Browning

Received: 25 August 2015 / Accepted: 8 April 2016 / Published online: 10 May 2016

Abstract
Context Arid rangelands have been severely degraded over the past century. Multi-temporal remote sensing techniques are ideally suited to detect significant changes in ecosystem state; however, considerable uncertainty exists regarding the effects of changing image resolution on their ability to detect ecologically meaningful change from satellite time-series.
Objectives (1) Assess the effects of image resolution in detecting landscape spatial heterogeneity. (2) Compare and evaluate the efficacy of coarse (MODIS) and moderate (Landsat) resolution satellite time-series for detecting ecosystem change.
Methods Using long-term (~12 year) vegetation monitoring data from grassland and shrubland sites in southern New Mexico, USA, we evaluated the effects of changing image support using MODIS (250-m) and Landsat (30-m) time-series in modeling and detecting significant changes in vegetation using time-series decomposition techniques.
Results Within our study ecosystem, landscape-scale (>20-m) spatial heterogeneity was low, resulting in a similar ability to detect vegetation changes across both satellite sensors and levels of spatial image support. While both Landsat and MODIS imagery were effective in modeling temporal dynamics in vegetation structure and composition, MODIS was more strongly correlated to biomass due to its cleaner (i.e., fewer artifacts/data gaps) 16-day temporal signal.
Conclusions The optimization of spatial/temporal scale is critical in ensuring adequate detection of change. While the results presented in this study are likely specific to arid shrub-grassland ecosystems, the approach presented here is generally applicable. Future analysis is needed in other ecosystems to assess how scaling relationships will change under different vegetation communities that range in their degree of landscape heterogeneity.

Keywords Time series · MODIS · Landsat · Image support · Arid ecosystems · Breaks for additive season and trend

Mention of a proprietary product does not constitute a guarantee or warranty of the products by the U.S. Government or the authors and does not imply its approval to the exclusion of other products that may be suitable.

Electronic supplementary material The online version of this article (doi:10.1007/s10980-016-0381-y) contains supplementary material, which is available to authorized users.

J. J. Maynard (✉) · J. W. Karl · D. M. Browning
USDA-ARS, Jornada Experimental Range, MSC 3JER,
New Mexico State University,
P.O. Box 30003, Las Cruces, NM 88003-8003, USA
e-mail: jmaynard@nmsu.edu

Introduction

Among the Earth's ecosystems, arid and semi-arid regions (~30 % of Earth's land area) have

experienced significant degradation over the past century due to intensive land-use practices (e.g., livestock overgrazing, recreation) and the increasing effects of drought and climate change. Many of these dryland ecosystems have experienced widespread displacement of perennial grasses by invasive shrubs, resulting in a significant reduction in important ecosystem services such as erosion control, carbon sequestration, and livestock forage (Bestelmeyer et al. 2015). Consequently, it is important to improve our understanding of how dryland ecosystems are responding to current management and climatic conditions. However, given the rate at which dryland systems are changing (Safriel et al. 2005), there is a critical need to develop methods that can detect changes in ecosystem properties and function in near-real time from local to regional scales.

Remote sensing is widely recognized as an important tool in detecting long-term landscape change and is capable of characterizing several classes of disturbance, including: (i) abrupt changes (e.g., deforestation, fires); (ii) gradual changes (e.g., prolonged drought, gradual land degradation); and (iii) seasonal changes (e.g., changing plant phenology due to intra-annual climatic variability or changing proportion of plant functional types) (Verbesselt et al. 2010b). While previous assessments of land cover change relied upon measurable difference between two satellite images (Coppin et al. 2004), current approaches are utilizing high temporal resolution image stacks to characterize temporal response functions (e.g., Kennedy et al. 2010; Verbesselt et al. 2010a; Wylie et al. 2012). These functions can provide information on the type of disturbance (e.g., fire, drought), the magnitude of the change (i.e., ecosystem resistance), the recovery or response of the system after disturbance (i.e., ecosystem resilience), and can be used to evaluate these temporal dynamics in relation to a historical baseline.

Recent technological and methodological advancements in the mapping and monitoring of land cover change are providing new opportunities for utilizing high temporal frequency satellite imagery (e.g., MODIS, Landsat). The most prominent among these include: (i) free and open distribution of imagery, allowing the creation of dense pixel-based time-series; (ii) significant advancements in image pre-processing (e.g., Landsat ecosystem disturbance adaptive processing system (LEDAPS) algorithm) creating comparable imagery across time; (iii) increases in computation capacity, in particular cloud-based computing platforms such as Google Earth Engine; and (iv) advances in change detection algorithms using high temporal resolution satellite image stacks (Kennedy et al. 2010; Verbesselt et al. 2010a, 2012). In light of these developments, a quantitative evaluation of the effects of spatial image support (e.g., Landsat vs. MODIS) on high temporal frequency change detection is needed.

Accurate detection of landscape change requires the optimization of spatial and temporal scales in remote sensing imagery to match the characteristic scale (i.e., typical spatial extent or temporal frequency that characterize an environmental pattern or process) of the phenomenon of interest (Wu and Li 2006; Kennedy et al. 2014). The effects of optimizing the spatial scale of remote sensing imagery have been well documented (Hay et al. 2001; Wu and Li 2006; Karl and Maurer 2010). Identifying an optimal pixel size is influenced by the spatial structure of the object of interest and the conditions required by the chosen analysis technique (Addink et al. 2007; Karl and Maurer 2010). The influence of these scaling effects in detecting landscape objects and their spatial characteristics can be interpreted using Strahler et al.'s (1986) two scene-resolution models for representing vegetation patterns in image data. Low-resolution (L-res) models apply where scene-elements are smaller than image pixels, and high-resolution (H-res) models apply where scene-elements are larger than image pixels. The application of these models is dependent, in part, upon the native resolution of the imagery relative to the characteristic scales of landscape objects. If the native image resolution is excessively coarse relative to the object of interest (L-res model), the ability to detect objects and patterns occurring at finer scales is limited. However, if the native image resolution is excessively fine relative to a landscape object (H-res model), an optimal pixel scale can be identified that matches the characteristic scale of the object using techniques such as average local variance (ALV) analysis (Woodcock and Strahler 1987).

The effects of the temporal scale or frequency of imagery on the ability to detect ecologically important biophysical changes of the Earth's surface (e.g., fires, insect damage, plant phenology) has been less studied. Previous limitations on computation capacity, a lack of sufficient analytical techniques, and financial constraints on image access, have historically

prevented studies from utilizing high temporal resolution image time-series. However, since landscape change occurs continuously through time, the ability to adequately characterize ecological change depends on the frequency of remote sensing measurements relative to the rate and shape of the response function (e.g., loss or growth of vegetation) (Kennedy et al. 2014). Conceptually, Strahler et al.'s (1986) spatial scene models can also be used to understand temporal scaling of remote sensing measurements. If the frequency of measurements is coarse relative to the studied phenomena (L-res model) it will fail to adequately characterize changes over time. Additionally, if the measurements have a very low signal-to-noise ratio (i.e., environmental factors affecting image quality or indicators with a low spectral response), then characterizing temporal response in a L-res model will be even more challenging due to the presence of artifacts, outliers, or a highly muted signal. Alternatively, measurements taken at a very high frequency relative to the studied phenomena (H-res model) will either accurately characterize its temporal dynamics (high signal-to-noise ratio) or contain excessive noise that must be filtered out by temporally scaling the time series before the rate and shape of the response function can be adequately defined.

The emergence of time-series decomposition techniques for uncoupling the seasonal and long-term signals from time-series image stacks, now allow for the detection of significant changes (i.e., abrupt, gradual, seasonal) in long term trends. The breaks for additive season and trend (BFAST) algorithm identifies seasonal and long-term trends in imagery time-series as well as significant changes (i.e., breakpoints) in modeled trends. BFAST integrates methods for change detection with the iterative decomposition of time-series into trend, seasonal, and noise components and can effectively separate seasonal and trend signals from noise and thus provides a method for optimizing temporal scale (Verbesselt et al. 2010a; see "Methods" section for greater detail). In contrast to temporal variability, vegetation exhibits a much higher degree of spatial variability due to a wide range of regulating controls, including edaphic, topographic and climatic factors that can vary across several orders of magnitude from meters to kilometers. Consequently, optimizing spatial image support is a more challenging task and requires an explicit understanding of characteristic scales, scaling domains (i.e., patch vs landscape), and how temporal response functions change across spatial scales.

While many studies have addressed the effect of spatial scale on the coupling of remote sensing and field-based data, simultaneous examinations of spatial and temporal scaling effects by coupling multi-temporal field data sets with time-series image stacks is lacking. To maximize quantitative detection of vegetation change, an optimal spatial resolution of satellite based time-series indices is needed. Consequently, the main objective of this study was to explicitly test the effects of changing image resolution on the ability of time-series indices to detect observed long-term (i.e., $\sim$12 years) changes in plant biomass. The optimal spatial resolution was then related to the spatial characteristics of the landscape, as well as the temporal response of seasonally measured biomass. Specific objectives were to (i) assess the effects of image resolution in detecting landscape spatial heterogeneity, and (ii) assess the utility of multi-temporal Landsat vs. MODIS imagery for detecting vegetation change using the BFAST change detection algorithm.

Study area

The study was conducted at the Jornada Basin Long Term Ecological Research (JRN) site in southern New Mexico, USA (32.5°N, 106.45°W). The JRN encompasses approximately 100,000 ha of semi-arid/arid grass-shrubland in the northern region of the Chihuahaun desert (Fig. 1). This study focused on two dominant ecosystem types within the study area: (1) upland grasslands dominated by black grama (*Bouteloua eriopoda* (Torr.) Torr.), mesa dropseed (*Sporobolus flexuosus* (Thurb. Ex Vasey) Rydb.), and several threeawn species (*Aristida* spp. L.); and (2) mesquite (*Prosopis glandulosa* Torr.) shrublands. Black grama grasslands are found on level locations with loamy sand to sandy loam soils, while mesquite shrublands are located on level uplands with loamy sand soils. Vast regions of southern New Mexico have transitioned from *Bouteloua*-dominated semi-desert grasslands to desert shrub (mesquite, creosote bush, and tarbush) ecosystems during the past 100 years (Gibbens et al. 2005; Browning et al. 2012). This pattern of conversion from grassland to shrubland has been well documented at the JRN (Browning et al. 2012) and is representative of patterns of vegetation transitions

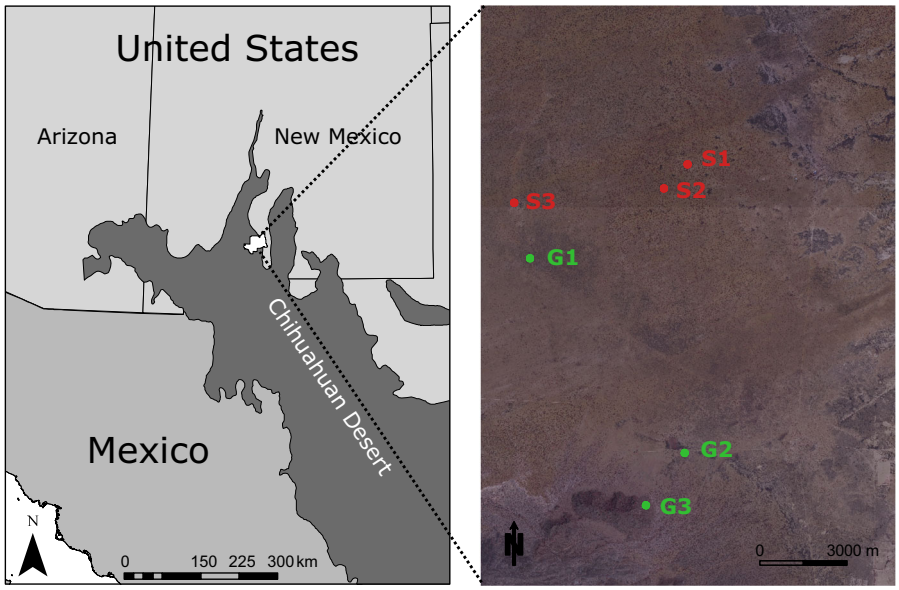

Fig. 1 Study site location in southwestern NM, USA and insert showing the location of the three grassland (G1–G3) and shrubland (S1–S3) sampling sites within the Jornada LTER

occurring in arid and semi-arid ecosystems globally resulting from long-term historical environmental change (Eldridge et al. 2011). The climate is arid to semiarid with mean annual precipitation of 25 cm over the past 30 years, with the majority of rainfall occurring between 1 July and 1 October. Mean monthly temperatures range from 6 °C in January to 26 °C in June, with an annual mean of 15 °C.

Methods

Field data collection

To examine how changing image support within satellite time-series affected the ability to detect vegetation change, we selected three upland grassland and three mesquite shrubland locations within the JRN (Fig. 1). Grassland and shrubland sites examined in this study are a subset of the JRN long-term ecosystem monitoring network established in 1989 that were initially established to encompass the range of natural variation within each ecosystem type. For example, in addition to differences in soils, geomorphic surface, and landscape position across all sites, grassland locations differed in abundance of the dominant black grama and shrublands exhibited a range of shrub sizes and densities. All study locations have been fenced since 1989 to exclude livestock. Each study location is comprised of a 7 × 7 grid of 49 permanent 1-m^2 quadrats, separated by 10-m in each cardinal compass direction. Within each quadrat, plant biomass was estimated nondestructively by measuring the dimensions (cover and height) of individual plants or plant parts (see Huenneke et al. 2001). Previously developed allometric equations were used to convert plant volume measurements to aboveground biomass. Biomass sampling occurred three times per calendar year (winter, spring, fall) between 2000 and 2012 to account for the distinctive seasonality of the Chihuahaun desert.

Time-series image acquisition and pre-processing

All available Landsat 5-Thematic Mapper (TM) imagery was acquired between 2000 and 2012 (16-day frequency), totaling 269 scenes (Path 33/Row 37). The Landsat imagery was ortho-corrected and radiometrically calibrated to surface reflectance with the LEDAPS algorithm (Masek et al. 2006). Cloud and cloud shadow masking were performed on all scenes using LEDAPS exclusion masks. Missing observations due to clouds, shadows or missing scenes (i.e.,

Landsat 5 scenes processed through NLAPS), were infilled using linear interpolation.

We acquired all available MODIS 250 m imagery (MOD13Q1) between 2000 and 2012 (16-day resolution), totaling 269 scenes (H09V05). The MOD13Q1 product is a 16-day composite which uses a constrained view-angle maximum value composite (CV-MVC) method. The CV-MVC method takes the highest quality value for each pixel within each 16-day window, thereby reducing anomalies associated with cloud cover and low sensor view angles (Huete et al. 2002). All images were corrected to surface reflectance, correcting for molecular scattering, ozone absorption, and aerosols. The MOD13Q1 product includes quality assurance (QA) flags with statistical data that indicate the quality of the indices and input data. The QA flags were used to only select cloud-free data of optimal quality. Missing data were replaced by linear interpolation within each pixel time series. MODIS data acquisition and preprocessing were performed using the 'MODIS' R package (version 0.10-11).

Normalized difference vegetation index (NDVI) is the most commonly used band ratio in ecological research and has been widely used in rangeland studies, although with varying levels of success (Anderson et al. 1993; Wylie et al. 2002; Sankey and Weber 2009). NDVI measurements are influenced by vegetation structure, texture and shadow and thus are indirectly correlated with above ground biomass (AGB) (Eisfelder et al. 2012). Numerous studies have successfully correlated maximum NDVI and/or time-integrated NDVI to AGB in arid ecosystems using both coarse scale (Sannier et al. 2002; Verbesselt et al. 2006; Wessels et al. 2006) and moderate-scale (Anderson et al. 1993; Wylie et al. 2002; Samimi and Kraus 2004) imagery. The limitations of using NDVI in arid ecosystems have been well documented, including the effects of exposed soil, standing dead vegetation and litter on the spectral response (Huete 1988; Gao et al. 2000). Despite its limitations, we have chosen to use NDVI in this study due to its widespread use. Additionally, prior research in a semi-arid environment showed that the choice of vegetation index did not affect modeled output from the BFAST time-series decomposition algorithm (Watts and Laffan 2013). NDVI was calculated from the red and NIR band values using the standard formula of:

$$\mathrm{NDVI} = (\rho\mathrm{NIR} - \rho\mathrm{Red})/(\rho\mathrm{NIR} + \rho\mathrm{Red}) \quad (1)$$

NDVI was calculated using Eq. 1 for Landsat TM imagery. The MODIS MOD13Q1 product contains a precomputed NDVI layer.

For all 49 subplot locations within each of the 70×70 m^2 grassland and shrubland study sites, we extracted the pixel value that each subplot intersected on each image acquisition date, resulting in 49 pixel values per date. Due to the larger footprint of MODIS (250 m) all subplots fall within one or two pixels, resulting in one or two repeating pixel values across the 49 subplots. In contrast, nine to eighteen unique Landsat pixels intersect with the 49 subplots resulting in varying combinations of sampling intensities across the pixels depending on where the subplot grid falls (Figs. 2a, 3a, S1a–S4a). All 49 subplot pixel values are averaged producing a spatially weighted mean NDVI value per sampling date.

Landscape heterogeneity and spatial image support

A QuickBird satellite image was acquired over the study area on 01 May 2003. The QuickBird imagery has a panchromatic band (0.6-m ground resolution) and four multispectral bands (2.4-m ground resolution). To extend the possible spatial range of our analysis, images were pan sharpened using the principal component method in Erdas Imagine® 8.7., resulting in a final resolution of 0.6-m for all bands. NDVI was calculated for QuickBird imagery using Eq. 1.

To examine the effect of spatial image support in detecting landscape heterogeneity we used average local variance analysis (ALV). The ALV function is a graph of the mean local variance in an image as a function of the pixel size of the image (Woodcock and Strahler 1987). ALV analysis was calculated from the QuickBird imagery in three steps: (1) a series of images with increasing pixel size were created by mean resampling of the original pixels; (2) standard deviation was calculated within a 3×3 moving window across each resampled image; and (3) the mean standard deviation across the entire image (i.e., ALV) was plotted against the coarsened pixel size. These graphs were used to measure spatial structure in images, with the peak of maximal variance at a spatial

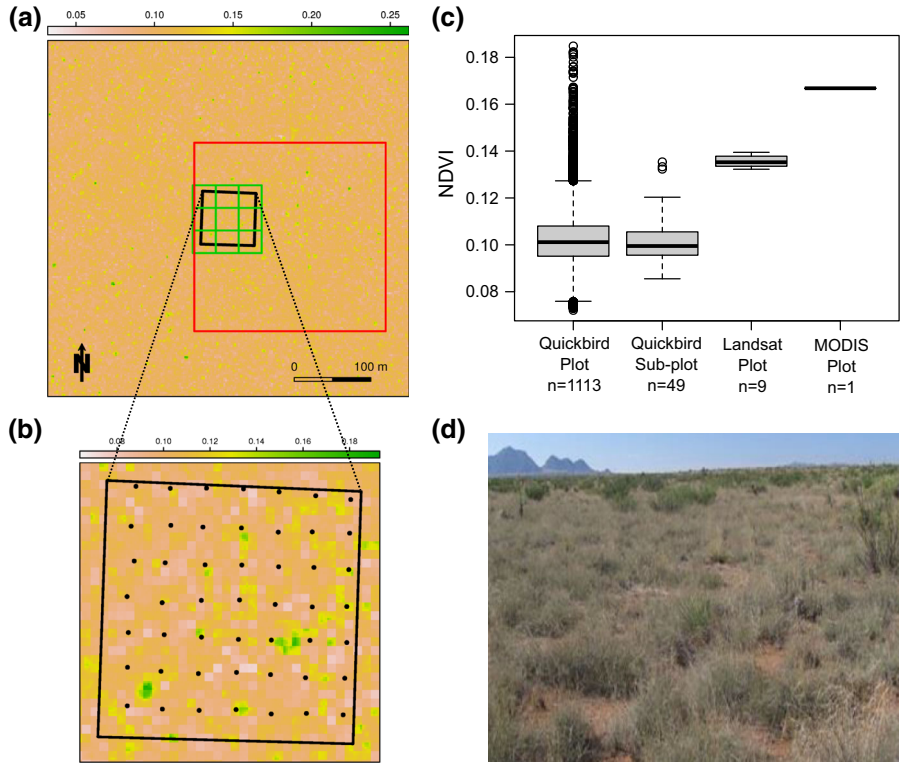

Fig. 2 Schematic of plot level variability at G1 showing: **a** the location of the 70 × 70 m^2 biomass sampling plot relative to the overlaying MODIS (n = 1) and Landsat (n = 9) pixels; **b** the biomass sampling plot and 49 1 × 1 m^2 biomass subplots, underlain by pan-sharpened Quickbird derived NDVI (0.6 m resolution); **c** a comparison NDVI variability for the entire plot (Quickbird plot), at the subplot locations (Quickbird subplot), and from the overlaying MODIS and Landsat pixels; and **d** a plot photo by D. Browning taken September 2009 illustrating fine-scale variability in vegetative cover

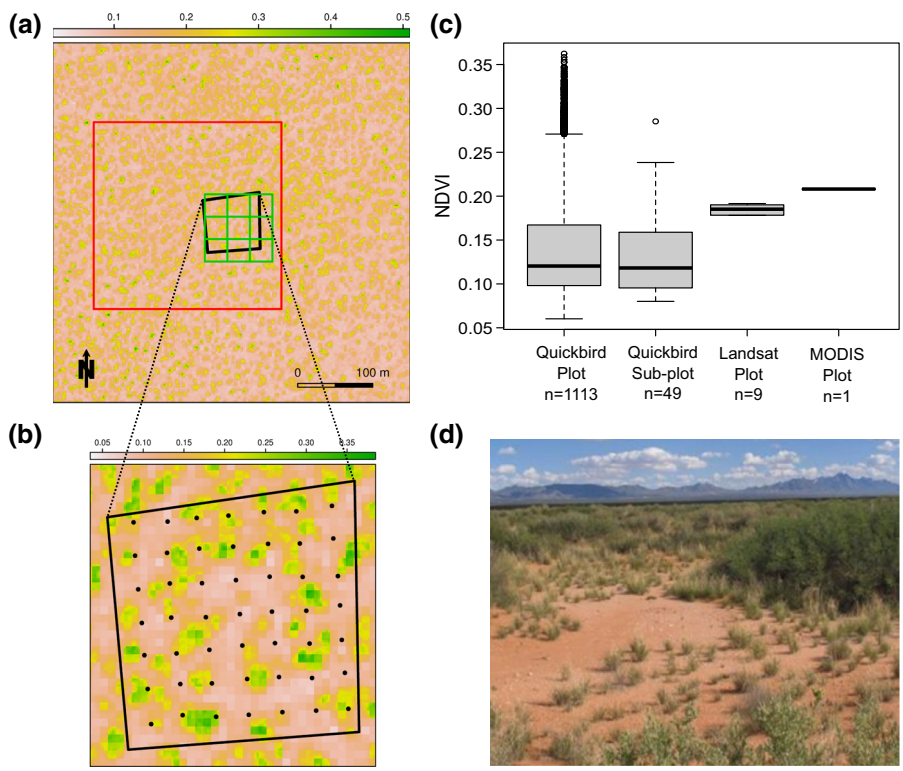

Fig. 3 Schematic of plot level variability at S1 showing: **a** the location of the 70 × 70 m^2 biomass sampling plot relative to the overlaying MODIS (n = 1) and Landsat (n = 9) pixels; **b** the biomass sampling plot and 49 1 × 1 m^2 biomass subplots, underlain by pan-sharpened Quickbird derived NDVI (0.6 m resolution); **c** a comparison NDVI variability for the entire plot (Quickbird plot), at the subplot locations (Quickbird subplot), and from the overlaying MODIS and Landsat pixels; and **d** a plot photo by D. Browning taken September 2009 illustrating fine-scale variability in vegetative cover

resolution that is closely related to the dominant size of pattern elements in the image (Woodcock and Strahler 1987; Nijland et al. 2009). In their analysis of satellite imagery from different sensors (e.g., Landsat, SPOT, AVHRR) and from different land cover classes (e.g., forest, agriculture, urban), Woodcock and Strahler (1987) found that the ALV function peaked at half to three quarters of the object size in the image. The ALV function can thus be used to quantify the spatial variability of a landscape, determine the source of variability (i.e., landscape component) and determine an optimal pixel size. ALV analysis is easy to calculate and interpret relative to alternative measures of image variance and spatial structure (e.g. geostatistical regularization), thus making it a suitable metric for the purposes of this study. Mean resampling of pan-sharpened QuickBird imagery was coarsened at 2-m increments from 2 to 40 m and 10-m increments from 50 to 1000 m; and standard deviation calculated within a 3 × 3 moving window for each image using the 'raster' package for R (Hijmans and van Etten 2014) (version 2.2-31).

Statistical analysis

We calculated a time-integrated NDVI (NDVI-I) on a per-pixel basis by summing all NDVI values for each period between biomass sampling events, resulting three NDVI-I values per year (i.e., dormant late winter: October–February; spring peak growth: March–May; and Fall peak growth: June–September). Each sum was divided by the number of NDVI observations within each sampling period to report NDVI-I values on the more familiar −1 to 1 NDVI scale. Landsat imagery was coarsened using mean resampling from its native 30 m resolution to 90, 240, 480 and 990 m; and MODIS was coarsened from its native 250 m resolution to 500 and 1000 m. An ordinary least-squares regression model was fit between the biomass and NDVI-I time-series with increasing spatial support size, to determine the optimal resolution for estimating biomass from NDVI imagery.

Satellite time-series decomposition

Time series decomposition was performed using the BFAST algorithm, implemented using the 'bfast' package for R (Verbesselt et al. 2010a) (version 1.5.7). The BFAST algorithm implements an additive decomposition of a time series into trend, seasonal and noise components through iteratively fitting a piecewise linear trend and seasonal model. The BFAST algorithm also has methods for detecting and characterizing abrupt changes (i.e., breaks) within both the trend and seasonal components. A test for the presence of abrupt changes in the data is performed prior to estimating the seasonal and trend components using an ordinary least squares (OLS) residuals-based moving sums (MOSUMs) test (Zeileis and Kleiber 2005). If a significant change is detected at a given alpha, the optimal number and position of breakpoints within the time series are returned based on the method of Bai and Perron (2003). The magnitude and direction of breaks are calculated from the intercept and slope of the trend component model and can occur at different times in the trend and seasonal components. For additional details on BFAST and model equations, see the SI Methods section.

A near-real time season-trend model for detecting significant disturbance in a satellite time-series representing both gradual and phenological changes was developed by Verbesselt et al. (2012). In this method, termed BFAST-Monitor, disturbances are detected within newly acquired time-series data (i.e., monitoring period) by automatically identifying a stable historical period (i.e., history period) to model the season-trend variation against which disturbances are detected.

Once the season-trend model is fit to a stable historical period, a MOSUM test is used to test whether all newly acquired data conforms to the existing model. The model is stable if the MOSUM process stays close to zero, however, if it deviates systematically from zero a structural break can occur (Verbesselt et al. 2010b). In this study, we set the history period between 2000 and 2003, as this was a relatively stable drought period characterized by abnormally low rainfall. In contrast, the monitoring period (2004–2012) was characterized by a period of abnormally wet years (2004–2010), followed by a return to dry conditions (2011–2012). Since the objective of this study was to evaluate the effects of changing image support on the ability to detect observed long-term changes in ecosystem properties, the selection of an abnormal (i.e., drought) period as our baseline (i.e., history period) was not an issue for this study. Our selection of the history period from 2000 to 2003 provided a 3–4 year stable baseline from

which subsequent changes (i.e., significant greening from 2004 to 2010) could be evaluated, thus allowing us to compare model results from both Landsat and MODIS sensors. For additional details on BFAST-Monitor and model equations, see the SI Methods section.

Results

Aboveground biomass estimation

Mean annual aboveground biomass (AGB) between 2000 and 2012 ranged from 48 to 412 g m^{-2} at grassland sites and from 62 to 422 g m^{-2} at shrubland sites (Fig. S5). Peak biomass usually occurred in the fall at grassland sites, while shrubland sites generally experienced peak biomass during spring sampling dates.

Plot level variability

Pan-sharpened QuickBird NDVI imagery of each grassland/shrubland plot revealed adequate discrimination between land cover types (e.g., shrubs, grasses, bare soil interspaces). For example, in the grassland sites, patches of bare soil (NDVI: 0.02–0.08) were intermixed with patches of black gramma grass (NDVI: 0.08–0.12), and the occasional shrub or succulent (NDVI: 0.12–0.18) (Figs. 2b, S1b, S2b). These patterns can be visually seen in the site photographs (Figs. 2d, S1d, S2d). In the shrubland sites, clear delineations can be made between shrubs (NDVI: 0.2–0.45) and bare soil interspaces (NDVI: 0.05–0.15) (Figs. 3b, S3b, S4b), which is further confirmed through visual assessment of site photographs (Figs. 3d, S3d, S4d).

To evaluate the effectiveness of the 49 1 × 1 m^2 sub-plots in characterizing the 70 × 70 m^2 within plot variability, we compared the distribution of all pan-sharpened QuickBird NDVI values within the main plot (n = 1113) to the NDVI values within the 49 subplots (n = 49). In general, the distribution of the 49 subplots had a similar median value and interquartile range to the distribution of all values within the main plot, indicating that the subplot sampling adequately characterized the within plot variability (Figs. 2c, 3c, S1c–S4c). The distributions of Landsat pixels (acquired on 5/10/2003) that intersect with the biomass plots had a small interquartile range, with NDVI values appreciably higher relative to QuickBird imagery. MODIS imagery (acquired on 5/09/2003) only intersected biomass plots with 1–2 pixels and had higher value(s) relative to either Landsat or QuickBird imagery. MODIS imagery covered ~9–18 times the area of the biomass plots and thus was detecting the average NDVI signal over a much larger extent.

Average local variance analysis

In general, ALV decreased rapidly from the 0.6 m resolution of the pan-sharpened QuickBird imagery, reaching a minimum by 30–50 m (Figs. 4, S6). The smallest pixel size corresponded to the highest ALV, thus indicating that the dominant patch size of landscape elements was less than or equal to the 0.6 m QuickBird imagery. Visual inspection of NDVI values across each biomass plot (Figs. 2, 3, S1–S4) showed a coarse but adequate delineation of landscape elements (e.g., shrubs, grasses, bare soil interspaces). For all three shrubland sites the ALV reached a minimum at a pixel size of 20–50 m and then remained constant as the pixel size was gradually coarsened out to 1000 m, indicating that both Landsat and MODIS imagery were characterizing the same degree of landscape heterogeneity and were thus operating at a similar landscape scale (Figs. 4, S6). The three grassland sites, however, showed different

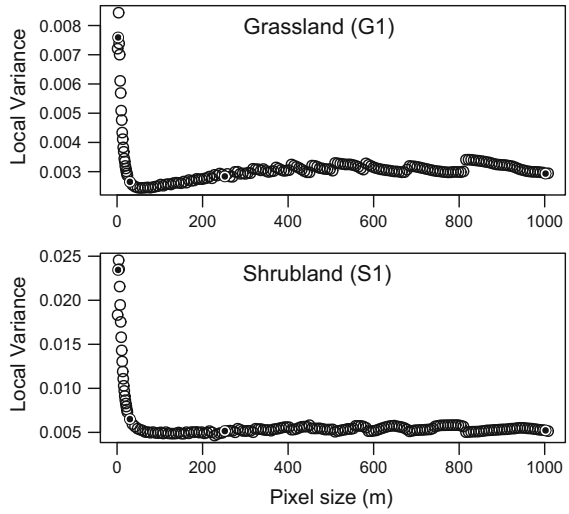

Fig. 4 Average local variance (ALV) analysis at G1 and S1 across a spatial range extending from 0.6 to 1000 m

patterns in ALV with increasing pixel size. While G1 followed a similar pattern to the shrubland sites, G2 and G3 showed a gradual increase in ALV following a minimum at ~40-m, with G2 continuing to increase up to 1000 m and G3 beginning to decline again between 800 and 1000 m (Figs. 4, S6). In general, shrubland sites had 2–3 times higher maximum ALV (ALV max: 0.020–0.025) relative grassland sites (ALV max: 0.008–0.016), with the exception of S3 which had a maximum ALV similar to the grassland sites (ALV max: 0.009) due to sparse shrub cover (Fig. S4b). This higher fine-scale spatial heterogeneity (i.e., <20-m) at shrubland sites is also shown by the wider interquartile range of QuickBird NDVI values relative to grassland sites (Figs. 2c, 3c).

Regression analysis of NDVI-biomass relationships

In this study, both Landsat and MODIS products were standardized to a 16 day temporal frequency. With Landsat, only one image was acquired within each 16-day period, whereas with the MODIS CV-MVC, a maximum of 64 images were acquired resulting in the highest quality image during that period. Consequently, Landsat time-series contain many sections of missing values due to periods of poor image quality. Landsat time-series were missing 27 % (n = 72) and 30 % (n = 80) of observations at G1 and S1, respectively (Fig. 5; Table 1). The other grassland and shrubland sites were missing between 29 and 31 % of observations (Fig. S7; Table 1). Despite missing values, visual comparison between Landsat and MODIS NDVI time-series showed good correspondence between inter-annual fluctuations (Fig. 5).

The strength of the relationship between biomass and NDVI-I was relatively invariant with increasing spatial support across all three grassland and shrubland sites (Fig. 6). Correlations between biomass and MODIS NDVI-I were consistently higher (r^2: ~0.3–0.5) than biomass ~ Landsat NDVI-I correlations (r^2: ~0.2–0.3) (Table 1). In general, MODIS produced stronger biomass ~ NDVI-I correlations at shrubland sites. However, Landsat produced similar correlations across both shrubland and grassland sites. Considerable variation existed in the correspondence between biomass correlations from MODIS and Landsat at each site. For example, MODIS and Landsat gave very similar coefficients of determination (r^2) at G1 (Fig. 6a), while MODIS has appreciably higher r^2 relative to Landsat at S1 (Fig. 6d). When all sites were combined, however, biomass ~ NDVI-I relationships were similar for both MODIS and Landsat, with r^2 of 0.45 and 0.41 for MODIS and Landsat, respectively (Table 1).

Time-series decomposition

BFAST decomposition of the NDVI time-series for G1 (Fig. 7a, b) and S1 (Fig. 7c, d) revealed similar linear models of the trend fitted to both Landsat and MODIS. Three significant breaks in the modeled trend were identified at G1 and one significant trend break identified at S1. Seasonal models, however, differed between MODIS and Landsat; with one significant seasonal break in the MODIS time-series at G1 and S1, and no seasonal breaks in the Landsat time-series at either site (Fig. 7). Similar dynamics were also observed at the other grassland and shrubland sites (Figs. S8, S9, respectively).

The effect of increasing spatial support on BFAST model results for Landsat and MODIS imagery can be seen in Fig. 8. The root mean squared error (RMSE) of residuals from BFAST models was relatively constant with increasing spatial support for both Landsat and MODIS (Fig. 8a, b). This indicates that within the spatial domain examined in this study (i.e., 30- to 1000-m), the spatial resolution of our time-series image stacks does not affect BFAST model results. This is confirmed by the detection of significant breaks in the trend component of BFAST models, where the number and timing of breaks is shown across a range of spatial support for Landsat (ls) and MODIS (m) at grassland (Fig. 8c) and shrubland (Fig. 8d) sites. Grassland sites show highly consistent breaks across all sites, sensors, and levels of image support. Shrubland sites display slightly greater variability in the number and timing of breaks, although consistent patterns are still clear.

To determine the effects of satellite sensor and spatial support in detecting land cover change, we examined spatial patterns in the magnitude and timing of significant changes across our study site utilizing the BFAST-Monitor algorithm. Similar patterns in the magnitude of change were detected from both Landsat (Fig. 9a) and MODIS (Fig. 9b) sensors, with 97 and

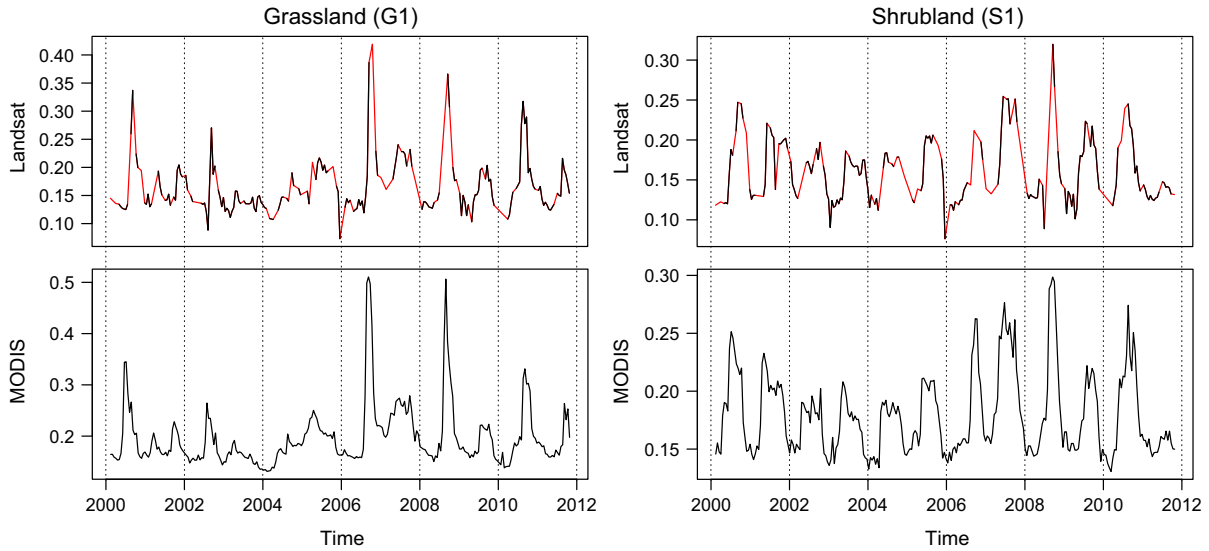

Fig. 5 Comparison of temporal variability in the NDVI time-series between Landsat and MODIS at G1 and S2 from 2000 to 2012. Segments of the Landsat NDVI time-series drawn in red indicate periods of missing data where linear interpolation was used to infill missing values

Table 1 Coefficients of determination (r^2) for linear regressions of seasonally measured biomass and time-integrated NDVI, shown at each grassland (G1–G3) and shrubland (S1–S3) site, across all grassland (G-All) and shrubland (S-All) sites, and across all sites (All). The percentage of each 12-year time-series that required linear infilling is also shown

Support m	G1	G2	G3	G-All r^2	S1	S2	S3	S-All	All
	Landsat								
30	0.34	0.17	0.20	0.15	0.19	0.27	0.30	0.24	0.16
90	0.34	0.17	0.21	0.16	0.20	0.27	0.34	0.26	0.17
240	0.41	0.21	0.18	0.18	0.20	0.27	0.24	0.24	0.17
480	0.40	0.16	0.22	0.20	0.22	0.32	0.25	0.26	0.18
990	0.41	0.19	0.16	0.20	0.20	0.35	0.31	0.28	0.23
	MODIS								
250	0.45	0.39	0.35	0.27	0.51	0.54	0.52	0.52	0.24
500	0.45	0.41	0.33	0.27	0.52	0.53	0.53	0.51	0.25
1000	0.45	0.42	0.32	0.27	0.52	0.52	0.50	0.51	0.35
				% Infill[†]					
MODIS	0	0	0	0	0	0	0	0	0
Landsat	27	29	31	29	30	29	30	29	29

[†] Percentage of missing scenes infilled by linear interpolation

99 % of all breaks having positive magnitudes for Landsat and MODIS, respectively, because the baseline period (2000–2003) was one of the driest multi-year periods of recent record. Similar spatial patterns were also observed with the timing of breaks between Landsat (Fig. 9c) and MODIS (Fig. 9d). BFAST-Monitor results from Landsat had areas with higher magnitudes of change as well as change occurring in more recent years (i.e., >2008) relative to MODIS results. This is largely a result of the higher spatial

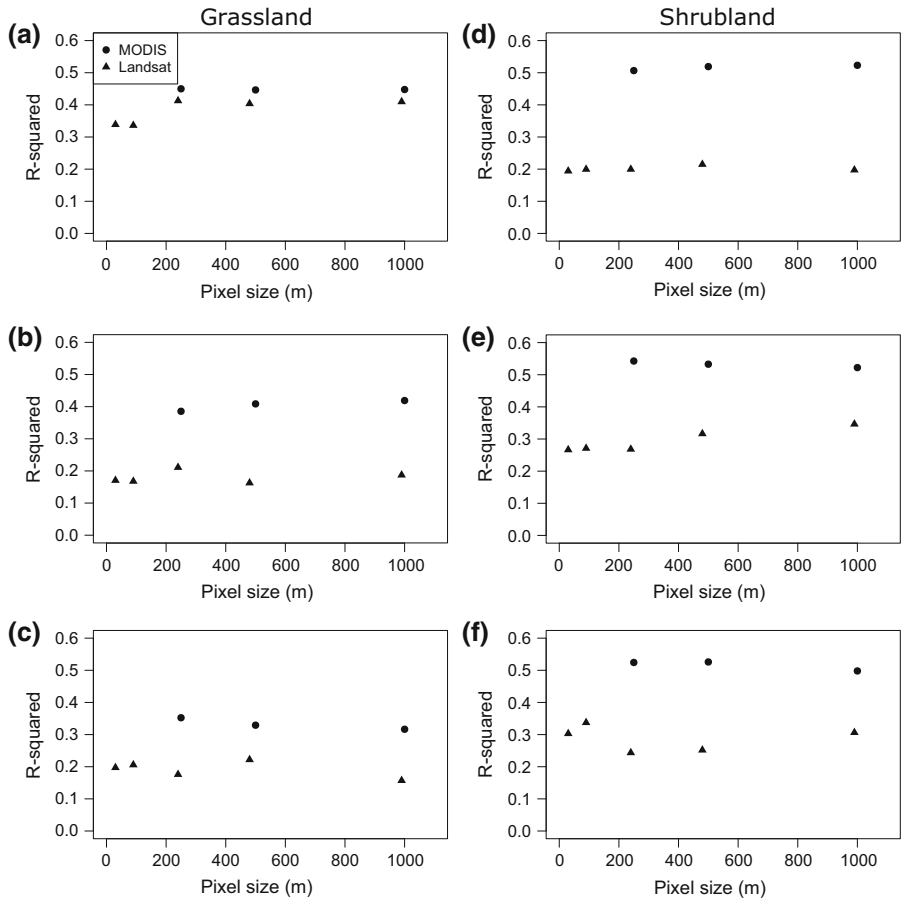

Fig. 6 Plots show the coefficients of determination (r2) from OLS regression models between biomass and NDVI-I time-series with an increasing spatial support size for the Landsat (30, 90, 240, 480 and 990 m) and MODIS (250, 500 and 1000 m) sensors at grassland [**a** G1, **b** G2, **c** G3] and shrubland [**d** S1, **e** S2, **f** S3] sites

resolution of Landsat which allows it to detect smaller areas of significant change (i.e., hotspots) that are muted within the larger pixel area of MODIS.

Discussion

Assessing landscape heterogeneity

The spatial structure of the study landscape as determined using ALV analysis of Quickbird imagery revealed two characteristic scales, the patch scale where individual landscape elements can be detected (i.e., shrubs and perennial grass patches, <1-m) and the landscape scale where the spectral signal from multiple landscape elements are averaged (>20-m). A previous assessment of patch scale (1-m^2) spatial heterogeneity at this site found that shrub-dominated systems had significantly greater heterogeneity in biomass relative to grass-dominated systems (Huenneke et al. 2002). Our results confirm these findings where shrublands had 2–3 times higher local variance at the patch scale relative to grassland sites. Differences in patch scale variability between sites within each ecosystem type are reflective of the initial study design where sites were selected to represent the range of natural variation. Thus variation in rainfall, landscape position, and soil properties are important drivers of patch scale variability.

At the landscape scale (>20-m) shrubland sites had consistently low local variance while grasslands sites were more variable, in particular study sites G2 and G3. The widespread conversion of perennial grasslands to desert shrublands at the JRN over the past

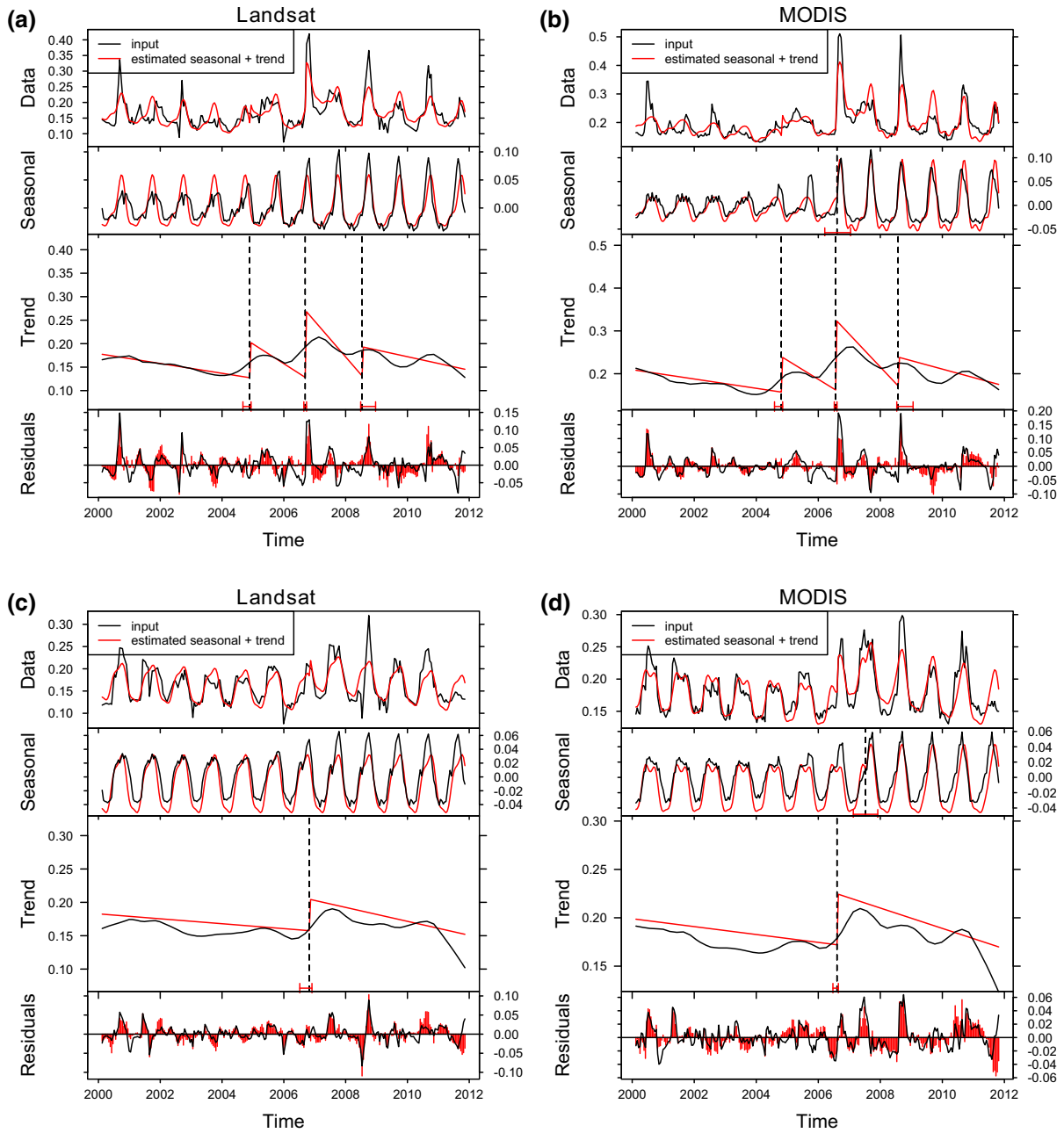

Fig. 7 Comparison of results from BFAST time series decomposition of the Landsat and MODIS time-series at G1 (**a**, **b**) and S1 (**c**, **d**). The time series data (*solid black line* in data panel) is the sum of the seasonal, trend and residuals time series. *Vertical dashed black lines* in either trend or seasonal panels indicate significant breaks in the time series

century has been well documented (Gibbens et al. 2005; Browning et al. 2012), resulting in remnant patches of native grasslands that have varying spatial extents. Grassland sites G2 and G3 are located on a different geomorphic landform (than site G1) on the southern portion of the JRN where grassland areas exist on landscapes with different potential for shrub proliferation. These fragmented grass-dominated areas result in increasing local variance as the image resolution increases and local variance calculations

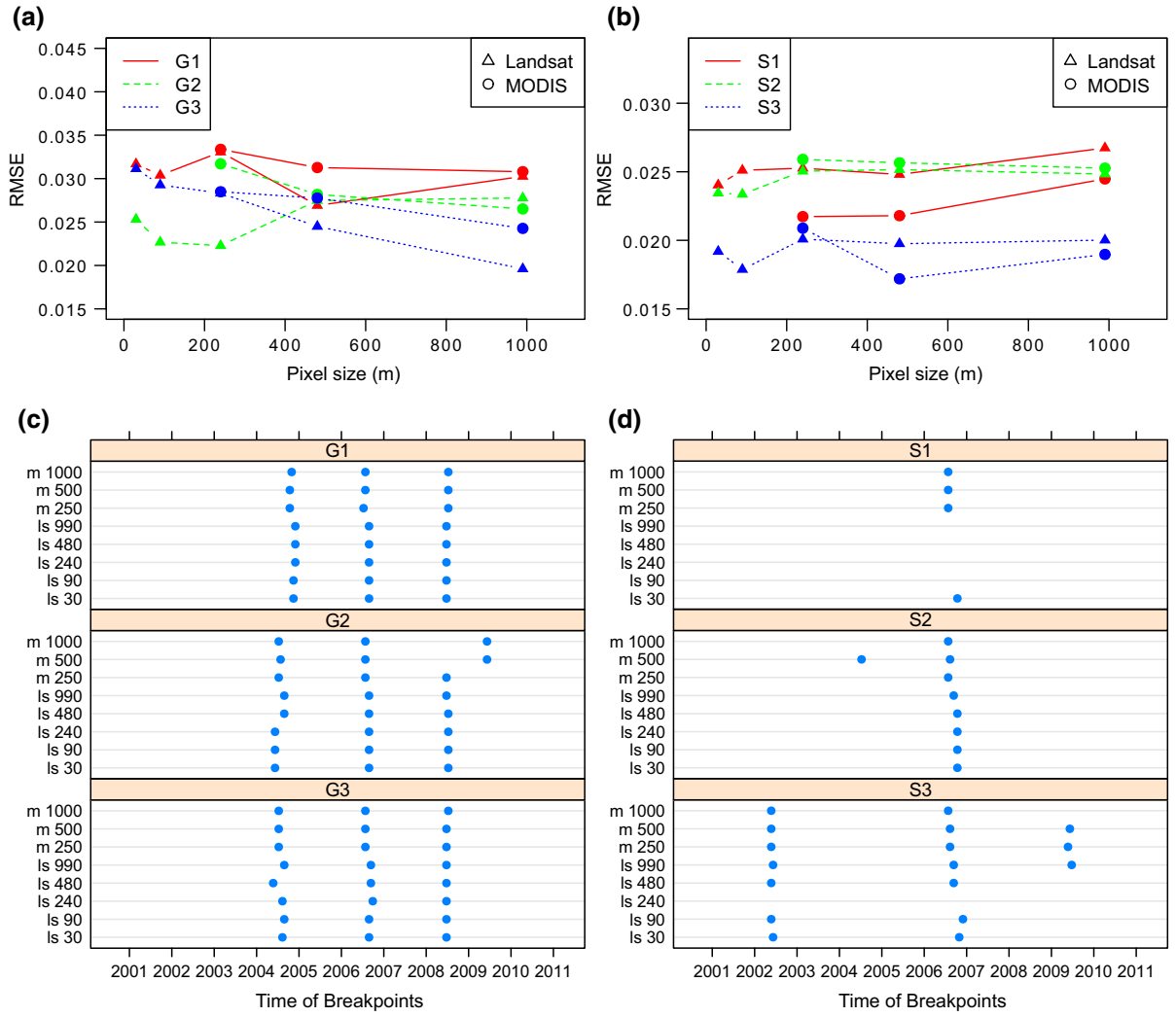

Fig. 8 Root mean square error of BFAST model residuals for Landsat and MODIS sensors across examined spatial image support at **a** grassland and **b** shrubland sites. Timing of significant trend breaks from BFAST models at **c** grassland and **d** shrubland sites

are made between pixels of contrasting vegetation composition.

Optimizing spatial image support for multi-temporal analysis

A fundamental premise in the estimation of biophysical properties using remotely sensed data is the existence of a predictable relationship between the spectral response measured by the sensor and the magnitude of the property of interest (Wulder et al. 2004). Several factors affect this relationship including the optical properties of the vegetation (e.g., vegetation structure, leaf spectral properties, area of bare soil), the effects caused by the spatial and temporal resolution of the sensor relative to the spatial structuring and temporal dynamics of the landscape, and finally environmental factors such as topography, sun elevation, haze, wind speed, and the view angle between the satellite and land surface. A common problem in validating remote-sensing based biomass estimates is the mismatch between the spatial resolution of the satellite data and the field plot size. Consequently, an important consideration when coupling remote sensing imagery with field-based data is the issue of registration error (i.e., misalignment of

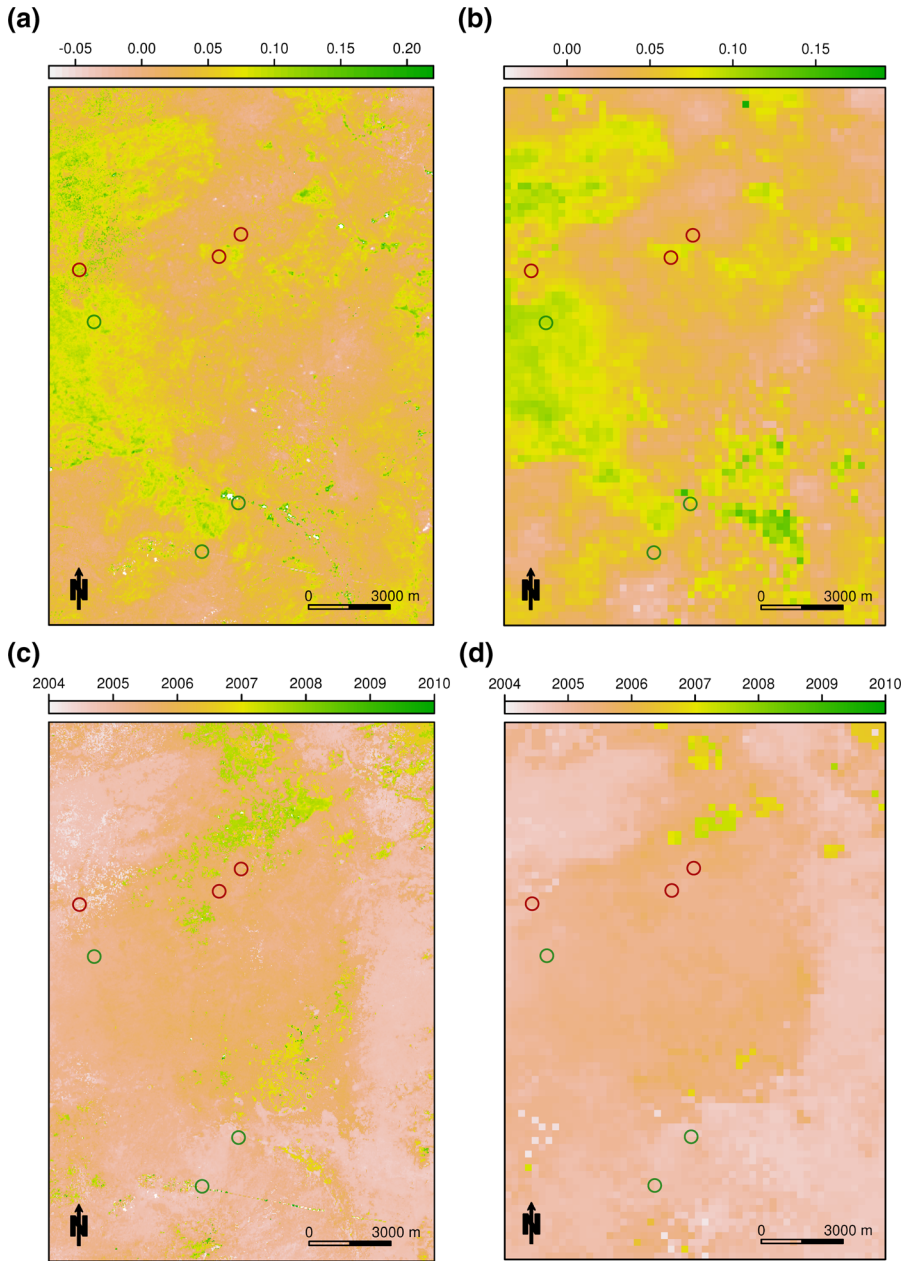

Fig. 9 Comparison of results from BFAST monitor for the Landsat (**a**, **c**) and MODIS (**b**, **d**) sensors, showing maps of **a**, **b** the magnitude of change (±) between 2004 and 2012, and **c**, **d** the year that significant change occurred

plot data and its corresponding remotely sensed image pixels). Registration errors can be particularly severe in highly heterogeneous landscapes. To account for plot level heterogeneity, previous studies have applied different field sampling strategies, including, transects (e.g., Sannier et al. 2002; Samimi and Kraus 2004; Wessels et al. 2006), nested sampling designs (e.g., Addink et al. 2007; Nijland et al. 2009), clustered measurement plots (e.g., Wylie et al. 1991; Sannier et al. 2002), and systematic grid sampling (e.g., Huenneke et al. 2001, 2002). In this study, the use of a systematic grid sampling design effectively characterized plot level variability (Figs. 2c, 3c). By extracting the intersecting pixel values corresponding to each of the 49 1-m biomass quadrats, a coarser resolution representation of the landscape was obtained, determined by the sensor resolution and the number of pixels aggregated. However, these aggregated spatial

scales still fell within our characterized spatial range (0.6–1000 m) and thus remained within the same scale domain.

We determined the optimal spatial resolution for detecting temporal changes in plant biomass by the spatial structure of the landscape and the temporal frequency of the time series for obtaining a high quality signal free of environmental contamination (e.g., clouds, atmospheric distortion). For our study ecosystem, ALV analysis indicated both Landsat and MODIS characterized the landscape scale and provided similar information on landscape structure. However, because Landsat is limited to a single observation within a 16-day cycle, it is highly susceptible to missing data resulting from environmental interference. In contrast, due to orbit overlap, the MODIS sensor can in theory collect a maximum of four observations per day or 64 observations within a 16-day cycle, and is thus able to extract the highest NDVI value within this period that has the smallest view angle (i.e., closest to nadir). Consequently, MODIS NDVI has a cleaner temporal signal and thus a better prediction of vegetation biomass.

Aboveground biomass estimation

Semi-arid and arid ecosystems express a high degree of temporal variability in vegetation distribution and dynamics in response to precipitation. Previous research has shown that NDVI time-series are closely related to rainfall dynamics in water limited ecosystems (Funk and Budde 2009; Vrieling et al. 2011). Additionally, vegetation communities have adapted different seasonal growth patterns; for example, shrublands consistently experience earlier (spring) peaks of production relative to grasslands (Huenneke et al. 2002). This high degree of intra-annual variability requires adequate temporal resolution to identify significant phenological changes in vegetation response. In this study, seasonally measured AGB allowed us to explicitly examine the relationship between intra-annual variability in AGB and NDVI-I derived from moderate (e.g., Landsat) and coarse (e.g., MODIS, AVHRR) resolution imagery. Several studies in arid ecosystems found strong correlations between AGB and both NDVI-I and maximum NDVI (Tucker et al. 1985; Wylie et al. 1991; Hobbs 1995), although these relationships have been shown to break down at low (i.e., <250 kg ha^{-1}) biomass levels (Tucker et al. 1985). Biomass levels within our study region fell within the lower range of values reported in the literature, with maximum annual values ranging between ~ 500 and 4000 kg ha^{-1} across all sites and the median of all maximum annual values falling below 2000 kg ha^{-1} at all sites. Correlations between NDVI-I and AGB in this study were not improved by restricting the range of biomass values to exclude low values (<250 kg ha^{-1}) within regression relationships.

Previous studies examining AGB in semi-arid environments have primarily focused on peak biomass within a single year or occasionally over multiple years. Few studies have examined either intra- or inter-annual changes in AGB and the ability of remote sensing to detect these changes. Strong inter-annual climatic variability in arid and semi-arid ecosystems can result in dramatic fluctuations in AGB between years. Using AVHRR data, Diouf and Lambin (2001) examined the relationship between annual NDVI-I and biomass over a 10-year period and concluded that, while separate regressions for each year resulted in good relationships, strong inter-annual variation resulted in a weak relationship between NDVI-I and biomass over the entire 10-year period. Wylie et al. (1991) observed similar results where strong inter-annual variability in drought conditions resulted in highly different relationships between NDVI-I and biomass in different years. Wessels et al. (2006) found NDVI-I produced relatively strong predictions of inter-annual variation in biomass at single sites, but failed to accurately predict biomass on an annual basis from all sites. In contrast to previous studies that have examined only inter-annual variability, this study examined both intra- and inter-annual variability in NDVI and biomass. Results from this study found that NDVI-I produced significant, although moderate-to-weak predictions of intra- and inter-annual variation in biomass both at individual sites, as well as across all sites using both moderate and course resolution imagery. High intra- and inter-annual variability in NDVI-I and biomass measurements likely resulted in the moderate to low coefficients of determination found in this study.

Assessing temporal frequency

The ability to detect significant changes (e.g., disturbance) within an NDVI time-series using the BFAST algorithm has been shown to be dependent upon the

signal-to-noise ratio (Verbesselt et al. 2012). Thus, adequate data preprocessing is necessary to improve the quality and reliability of remotely sensed time-series datasets for detection of significant landscape change. In this study we used a simple linear interpolation to fill data gaps within the Landsat time-series. In general, this simplistic approach provided a complete time-series that corresponded well with the higher quality MODIS time-series, however, correlations between Landsat and seasonal biomass were often appreciably lower than correlations between MODIS and seasonal biomass. Lower correlations between seasonal biomass and Landsat were likely the result of the infilling process and/or the fact that for any 16-day period MODIS produces a higher-quality set of data via the CV-MVC.

Several data fusion techniques have been developed to deal with missing data or to increase the frequency of satellite time-series by linking MODIS and Landsat sensor data (Gao et al. 2006; Sedano et al. 2014). Among these data fusion techniques, the spatial and temporal adaptive reflectance fusion model (STARFM) (Gao et al. 2006; Hilker et al. 2009; Schmidt et al. 2012) and Kalman filtering (Sedano et al. 2014) have been successfully used to both increase the temporal frequency and improve the temporal signal (i.e., removing environmental artifacts) of moderate resolution sensors such as Landsat. Time-series of synthetic NDVI images derived from the STARFM and Kalman filter methods were shown to capture seasonal land surface dynamics while maintaining the spatial structure of the landscape but at a higher spatial resolution (Schmidt et al. 2012; Sedano et al. 2014). Data fusion techniques provide new opportunities to examine land surface processes at more ecologically relevant scales. Future work at the JRN using data fusion techniques is needed given the large number of data gaps ($\sim$30 %) within the Landsat time series resulting from periods of cloud cover.

Implications for monitoring ecosystem change

The spatial resolution of satellite imagery is important in the ability to quantify landscape change, for it affects both the degree to which landscape features can be differentiated and the strength of the relationship between satellite imagery and field data. The importance of spatial scale, however, is largely dependent upon the spatial heterogeneity of the landscape. Results from this study showed that both Landsat and MODIS performed similarly in terms of modeling temporal shifts in vegetation composition. In landscapes of greater heterogeneity where vegetation composition varies over smaller scales, greater differences may occur between Landsat and MODIS imagery as MODIS pixels span multiple ecosystem types. Thus while Landsat cannot provide real time monitoring of ecosystem change across broad extents due to its long repeat interval (16–18 days), with its long data record (1972-present) and high spatial resolution it is capable of detecting subtle environmental changes that would be missed by coarser spatial resolution satellites (Kerr and Ostrovsky 2003).

Vegetative composition of the land surface has been shown to influence the utility of remotely sensed imagery as a proxy for surface properties. For example, Sankey and Weber (2009) found that when bare ground reached or exceeded 20 %, SPOT derived NDVI was no longer statistically significant as a predictor variable for biomass in two semi-arid rangeland ecosystems. This was likely the result of a low signal-to-noise ratio, since the seasonal amplitude in NDVI decreases with increasing bare ground and the SPOT imagery acquired was from a single date rather than a higher quality composite. The BFAST algorithm is a signal-to-noise driven method which analyzes the full time-series and detects abnormal changes based on the signal versus noise distribution (Verbesselt et al. 2012). Thus in areas where the seasonal amplitude in NDVI is low (i.e., <0.1) due to a high percentage of bare ground, the ability to detect significant change is reduced. This is particularly problematic when the noise level (e.g., from clouds, atmospheric distortion) is high as is the case in satellites with coarse temporal resolution (e.g., Landsat).

Conclusions

Recent developments in remote sensing, including advances in data access, data preprocessing, analytical techniques, and computational capacity have greatly improved the ability to detect and quantify landscape change. While these advancements provide new opportunities for understanding ecosystem changes at finer spatial and temporal resolutions, there is still a

critical need to understand the effects of scale (i.e., spatial and temporal) on modeled results and select scales optimal for stated monitoring and management objectives. Within our study area, ALV analysis revealed two characteristic scales: patch scale (<1 m) and landscape scale (>20 m). Thus the optimal spatial scale for detecting vegetation patch structure in this grass-shrub ecosystem was determined to be less than 1 m and that by 30 m the spatial variability was minimized resulting in each pixel characterizing the average landscape structure. To accurately correlate satellite time series to field data, the spatial variability must be similar at both the resolution of the satellite sensor and spatial scale of the field sampling. Our use of a systematic grid sampling design effectively characterized each plot at the landscape scale. While both Landsat and MODIS imagery were effective in modeling temporal dynamics in vegetation structure and composition, MODIS was more strongly correlated to biomass measurements due to its higher temporal resolution, thus producing a cleaner 16-day temporal signal upon compositing (CV-MVC). Advances in multi-temporal remote sensing are resulting in a more refined quantification of landscape change aligned with ecological concepts and models, but the optimization of spatial and temporal scale is critical in ensuring adequate detection of change. While the results presented in this study are likely specific to the ecosystem type it represents (i.e., arid shrub-grasslands), the approach presented here is generally applicable. Future analysis is needed in other ecosystems to assess how scaling relationships will change under different vegetation communities that range in their degree of landscape heterogeneity.

References

Addink E, De Jong S, Pebesma E (2007) The importance of scale in object-based mapping of vegetation parameters with hyperspectral imagery. Photogramm Eng Remote Sens 73:905–912

Anderson G, Hanson J, Haas R (1993) Evaluating landsat thematic mapper derived vegetation indices for estimating above-ground biomass on semiarid rangelands. Remote Sens Environ 45:165–175

Bai J, Perron P (2003) Computation and analysis of multiple structural change models. J Appl Econom 18:1–22

Bestelmeyer BT, Okin GS, Duniway MC, Archer SR, Sayre NF, Williamson JC, Herrick JE (2015) Desertification, land use, and the transformation of global drylands. Front Ecol Environ 13:28–36

Browning DM, Duniway MC, Laliberte AS, Rango A (2012) Hierarchical analysis of vegetation dynamics over 71 years: soil-rainfall interactions in a Chihuahuan Desert ecosystem. Ecol Appl 22:909–926

Coppin P, Jonckheere I, Nackaerts K, Muys B, Lambin E (2004) Digital change detection methods in ecosystem monitoring: a review. Int J Remote Sens 25:1565–1596

Diouf A, Lambin EF (2001) Monitoring land-cover changes in semi-arid regions: remote sensing data and field observations in the Ferlo, Senegal. J Arid Environ 48:129–148

Eisfelder C, Kuenzer C, Dech S (2012) Derivation of biomass information for semi-arid areas using remote-sensing data. Int J Remote Sens 33:2937–2984

Eldridge DJ, Bowker MA, Maestre FT, Roger E, Reynolds JF, Whitford WG (2011) Impacts of shrub encroachment on ecosystem structure and functioning: towards a global synthesis. Ecol Lett 14:709–722

Funk C, Budde ME (2009) Phenologically-tuned MODIS NDVI-based production anomaly estimates for Zimbabwe. Remote Sens Environ 113:115–125

Gao X, Huete AR, Ni W, Miura T (2000) Optical-biophysical relationships of vegetation spectra without background contamination. Remote Sens Environ 74:609–620

Gao F, Masek J, Schwaller M, Hall F (2006) On the blending of the landsat and MODIS surface reflectance: predicting daily landsat surface reflectance. IEEE Trans Geosci Remote Sens 44:2207–2218

Gibbens RP, McNeely RP, Havstad KM, Beck RF, Nolen B (2005) Vegetation changes in the Jornada Basin from 1858 to 1998. J Arid Environ 61:651–668

Hay G, Marceau D, Dube P, Bouchard A (2001) A multiscale framework for landscape analysis: object-specific analysis and upscaling. Landscape Ecol 16:471–490

Hijmans RJ, van Etten J (2014) raster: Geographic data analysis and modeling. R Packag. version 2.3-12. http://CRAN.R-project.org/package=raster

Hilker T, Wulder MA, Coops NC, Linke J, McDermid G, Masek JG, White JC (2009) A new data fusion model for high spatial- and temporal-resolution mapping of forest disturbance based on Landsat and MODIS. Remote Sens Environ 113:1613–1627

Hobbs TJ (1995) The use of NOAA-AVHRR NDVI data to assess herbage production in the arid rangelands of Central Australia. Int J Remote Sens 16:1289–1302

Huenneke LF, Anderson JP, Remmenga M, Schlesinger WH (2002) Desertification alters patterns of aboveground net primary production in Chihuahuan ecosystems. Glob Chang Biol 8:247–264

Huenneke LF, Clason D, Muldavin E (2001) Spatial heterogeneity in Chihuahuan Desert vegetation: implications for sampling methods in semi-arid ecosystems. J Arid Environ 47:257–270

Huete A (1988) A soil-adjusted vegetation index (SAVI). Remote Sens Environ 25:295–309

Huete A, Didan K, Miura T, Rodriguez EP, Gao X, Ferreira LG (2002) Overview of the radiometric and biophysical performance of the MODIS vegetation indices. Remote Sens Environ 83:195–213

Karl JW, Maurer BA (2010) Spatial dependence of predictions from image segmentation: a variogram-based method to determine appropriate scales for producing land-management information. Ecol Inform 5:194–202

Kennedy RE, Andréfouët S, Cohen WB, Gómez C, Griffiths P, Hais M, Meigs GW (2014) Bringing an ecological view of change to landsat-based remote sensing. Front Ecol Environ 12:339–346

Kennedy RE, Yang Z, Cohen WB (2010) Detecting trends in forest disturbance and recovery using yearly Landsat time series: 1. LandTrendr—temporal segmentation algorithms. Remote Sens Environ 114:2897–2910

Kerr JT, Ostrovsky M (2003) From space to species: ecological applications for remote sensing. Trends Ecol Evol 18:299–305

Masek JG, Vermote EF, Saleous NE, Wolfe R, Hall FG, Huemmrich KF, Lim TK (2006) A landsat surface reflectance dataset for North America, 1990–2000. IEEE Geosci Remote Sens Lett 3:68–72

Nijland W, Addink EA, De Jong SM, Van der Meer FD (2009) Optimizing spatial image support for quantitative mapping of natural vegetation. Remote Sens Environ 113:771–780

Safriel U, Adeel Z, Niemeijer DP, White R, Lal R, Winslow M, Ziedler J, Prince S, Archer E, Caroline K (2005) Dryland systems. In: Ecosystems and human well-being: current state and trends: findings of the condition and trends working group. pp 625–662

Samimi C, Kraus T (2004) Biomass estimation using Landsat-TM and -ETM+ . Towards a regional model for Southern Africa? GeoJournal 59:177–187

Sankey TT, Weber KT (2009) Rangeland assessments using remote sensing: is NDVI useful? In: Final report: comparing effects of management practices on rangeland health with geospatial technologies (NNX06AE47G). p 168

Sannier CAD, Taylor JC, Du Plessis W (2002) Real-time monitoring of vegetation biomass with NOAA-AVHRR in Etosha National Park, Namibia, for fire risk assessment. Int J Remote Sens 23:71–89

Schmidt M, Udelhoven T, Gill T, Röder A (2012) Long term data fusion for a dense time series analysis with MODIS and Landsat imagery in an Australian Savanna. J Appl Remote Sens 6:063512

Sedano F, Kempeneers P, Hurtt G (2014) A Kalman filter-based method to generate continuous time series of medium-resolution NDVI images. Remote Sens 6:12381–12408

Strahler AH, Woodcock CE, Smith JA (1986) On the nature of models in remote sensing. Remote Sens Environ 20:121–139

Tucker CJ, Vanpraet CL, Sharman MJ, Van Ittersum G (1985) Satellite remote sensing of total herbaceous biomass production in the Senegalese Sahel: 1980–1984. Remote Sens Environ 17:233–249

Verbesselt J, Hyndman R, Newnham G, Culvenor D (2010a) Detecting trend and seasonal changes in satellite image time series. Remote Sens Environ 114:106–115

Verbesselt J, Hyndman R, Zeileis A, Culvenor D (2010b) Phenological change detection while accounting for abrupt and gradual trends in satellite image time series. Remote Sens Environ 114:2970–2980

Verbesselt J, Somers B, Van Aardt J, Jonckheere I, Coppin P (2006) Monitoring herbaceous biomass and water content with SPOT VEGETATION time-series to improve fire risk assessment in savanna ecosystems. Remote Sens Environ 101:399–414

Verbesselt J, Zeileis A, Herold M (2012) Near real-time disturbance detection using satellite image time series. Remote Sens Environ 123:98–108

Vrieling A, de Beurs KM, Brown ME (2011) Variability of African farming systems from phenological analysis of NDVI time series. Clim Change 109:455–477

Watts LM, Laffan SW (2013) Sensitivity of the BFAST algorithm to MODIS satellite and vegetation index. In: Piantadosi J, Anderssen R, Boland J (eds) 20th International congress on modelling and simulation. Modelling and Simulation Society of Australia and New Zealand Inc., Adelaide, pp 1638–1644

Wessels KJ, Prince SD, Zambatis N, Macfadyen S, Frost PE, Van Zyl D (2006) Advanced very high resolution radiometer (AVHRR) NDVI in Kruger National Park, South Africa. Int J Remote Sens 27:951–973

Woodcock CE, Strahler AH (1987) The factor of scale in remote sensing. Remote Sens Environ 21:311–332

Wu J, Li H (2006) Concepts of scale and scaling. In: Wu J, Jones KB, Li H, Loucks OL (eds) Scaling and uncertainty analysis in ecology: methods and applications, 1st edn. Springer, Dordrecht, pp 3–15

Wulder MA, Hall RJ, Coops NC, Franklin SE (2004) High spatial resolution remotely sensed data for ecosystem characterization. Bioscience 54:511–521

Wylie BK, Boyte SP, Major DJ (2012) Ecosystem performance monitoring of rangelands by integrating modeling and remote sensing. Rangel Ecol Manag 65:241–252

Wylie BK, Harrington JA Jr, Prince SD, Denda I (1991) Satellite and ground-based pasture production assessment in Niger: 1986–1988. Int J Remote Sens 12:1281–1300

Wylie BK, Meyer DJ, Tieszen LL, Mannel S (2002) Satellite mapping of surface biophysical parameters at the biome scale over the North American grasslands a case study. Remote Sens Environ 79:266–278

Zeileis A, Kleiber C (2005) Validating multiple structural change models-a case study. J Appl Econom 20:685–690